

Transverse magneto-optical Kerr effect in subwavelength dielectric gratings

Ivan S. Maksymov,* Jessica Hutomo, and Mikhail Kostylev

School of Physics, University of Western Australia, 35 Stirling Hwy, Crawley 6009, Australia

*ivan.maksymov@uwa.edu.au

Abstract: We demonstrate theoretically a large transverse magneto-optical Kerr effect (TMOKE) in subwavelength gratings consisting of alternating magneto-insulating and nonmagnetic dielectric nanostripes. The reflectivity of the grating reaches 96% at the frequencies corresponding to the maximum of the TMOKE response. The combination of a large TMOKE response and high reflectivity is important for applications in 3D imaging, magneto-optical data storage, and magnonics.

© 2014 Optical Society of America

OCIS codes: (230.3810) Magneto-optic systems; (050.6624) Subwavelength structures.

References and links

1. A. K. Zvezdin and V. A. Kotov, *Modern Magneto-Optics and Magneto-Optical Materials* (IOP Publishing, Bristol, 1997).
2. Ken-ichi Aoshima, N. Funabashi, K. Machida, Y. Miyamoto, K. Kuga, T. Ishibashi, N. Shimidzu, and F. Sato, "Submicron magneto-optical spatial light modulation device for holographic displays driven by spin-polarized electrons," *J. Display Tech.* **6**, 374–380 (2010).
3. V.V. Kruglyak, S.O. Demokritov, and D. Grundler, "Magnonics," *J. Phys. D: Appl. Phys.* **43**, 264001 (2010).
4. A. A. Serga, A. V. Chumak, and B. Hillebrands, "YIG magnonics," *J. Phys. D: Appl. Phys.* **43**, 264002 (2010).
5. G. Armelles, A. Cebollada, A. García-Martín, and M. U. González, "Magnetoplasmonics: combining magnetic and plasmonic functionalities," *Adv. Opt. Mater.* **1**, 10–35 (2013).
6. G. A. Wurtz, W. Hendren, R. Pollard, R. Atkinson, L. Le Guyader, A. Kirilyuk, Th. Rasing, I. I. Smolyaninov, and A. V. Zayats, "Controlling optical transmission through magneto-plasmonic crystals with an external magnetic field," *New J. Phys.* **10**, 105012 (2008).
7. V. I. Belotelov, I. A. Akimov, M. Pohl, V. A. Kotov, S. Kasture, A. S. Vengurlekar, A. V. Gopal, D. R. Yakovlev, A. K. Zvezdin, and M. Bayer, "Enhanced magneto-optical effects in magnetoplasmonic crystals," *Nature Nanotechnol.* **6**, 370–376 (2011).
8. A. V. Chetvertukhin, A. A. Grunin, A. V. Baryshev, T. V. Dolgova, H. Uchida, M. Inoue, and A. A. Fedyanin, "Magneto-optical Kerr effect enhancement at the Wood's anomaly in magnetoplasmonic crystals," *J. Magn. Mater.* **324**, 3516 (2012).
9. N. Kostylev, I. S. Maksymov, A. O. Adeyeye, S. Samarin, M. Kostylev, and J. F. Williams, "Plasmon-assisted high reflectivity and strong magneto-optical Kerr effect in Py gratings," *Appl. Phys. Lett.* **102**, 121907 (2013).
10. V. I. Belotelov, L. E. Kreilkamp, I. A. Akimov, A. N. Kalish, D. A. Bykov, S. Kasture, V. J. Yallapragada, A. V. Gopal, A. M. Grishin, S. I. Khartsev, M. Nur-E-Alam, M. Vasiliev, L. L. Doskolovich, D. R. Yakovlev, K. Alameh, A. K. Zvezdin, and M. Bayer, "Plasmon-mediated magneto-optical transparency," *Nat. Commun.* **4**, 2128 (2013).
11. L. Halagačka, M. Vanwolleghem, K. Postava, B. Dagens, and J. Pištora, "Coupled mode enhanced giant magnetoplasmonics transverse Kerr effect," *Opt. Express* **21**, 21741–21755 (2013).
12. J. Chen, P. Albella, Z. Pirzadeh, P. Alonso-González, F. Huth, S. Bonetti, V. Bonanni, J. Åkerman, J. Nogués, P. Vavassori, A. Dmitriev, J. Aizpurua, and R. Hillenbrand, "Plasmonic nickel nanoantennas," *Small* **7**, 2341–2347 (2011).
13. V. Bonanni, S. Bonetti, T. Pakizeh, Z. Pirzadeh, J. Chen, J. Nogués, P. Vavassori, R. Hillenbrand, J. Åkerman, and A. Dmitriev, "Designer magnetoplasmonics with nickel nanoferrromagnets," *Nano Lett.* **11**, 5333–5338 (2011).
14. A. Hessel and A. A. Oliner, "A new theory of Wood's anomalies on optical gratings," *Appl. Opt.* **4**, 1275–1297 (1965).

15. S. S. Wang and R. Magnusson, "Theory and applications of guided-mode resonance filters," *Appl. Opt.* **32**, 2606–2613 (1993).
16. C. F. R. Mateus, M. C. Y. Huang, L. Chen, C. J. Chang-Hasnain, and Y. Suzuki, "Broad-band mirror (1.12 – 1.62 μ m) using a subwavelength grating," *IEEE Photon. Technol. Lett.* **16**, 1676–1678 (2004).
17. D. W. Peters, S. A. Kemme, and G. R. Hadley, "Effect of finite grating, waveguide width, and end-facet geometry on resonant subwavelength grating reflectivity," *J. Opt. Soc. Am.* **21**, 981–987 (2004).
18. J. R. Marciano and D. H. Raguin, "High-efficiency, high-dispersion diffraction gratings based on total internal reflection," *Opt. Lett.* **29**, 542–544 (2004).
19. E. Baisillon, D. Tan, B. Faraji, A. G. Kirk, L. Chrostowski, and D. V. Plant, "High reflectivity air-bridge subwavelength grating reflector and Fabry-Perot cavity in AlGaAs/GaAs," *Opt. Express* **14**, 2573–2582 (2006).
20. A. E. Miroshnichenko, S. Flach, and Yu. S. Kivshar, "Fano resonances in nanoscale structures," *Rev. Mod. Phys.* **82**, 2257–2298 (2010).
21. Y. Souche, V. Novosad, B. Pannetier, and O. Geoffroy, "Magneto-optical diffraction and transverse Kerr effect," *J. Magn. Magn. Mater.* **177–181**, 1277–1278 (1998).
22. B. Bai, J. Tervo, and J. Turunen, "Polarization conversion in resonant magneto-optic gratings," *New J. Phys.* **8**, 205 (2006).
23. H. Marinchio, R. Carminati, A. García-Martín, and J. J. Sáenz, "Magneto-optical Kerr effect in resonant subwavelength nanowire gratings," *New J. Phys.* **16**, 015007 (2014).
24. T. Amemiya, A. Ishikawa, Y. Shoji, Pham Nam Hai, M. Tanaka, T. Mizumoto, T. Tanaka, and S. Arai, "Three-dimensional nanostructuring in YIG ferrite with femtosecond laser," *Opt. Lett.* **39**, 212–215 (2014).
25. M. Pohl, L. E. Kreilkamp, V. I. Belotelov, I. A. Akimov, A. N. Kalish, N. E. Khokhlov, V. J. Yallapragada, A. V. Gopal, M. Nur-E-Alam, and M. Vasiliev, "Tuning of the transverse magneto-optical Kerr effect in magneto-plasmonic crystals," *New J. Phys.* **15**, 075024 (2013).
26. M. G. Moharam, E. B. Grann, D. A. Pomett, and T. K. Gaylord, "Formulation for stable and efficient implementation of the rigorous coupled-wave analysis of binary gratings," *J. Opt. Soc. Am. A* **12**, 1068–1076 (1995).

1. Introduction

The transverse magneto-optical (MO) Kerr effect (TMOKE) is defined as a change of reflected intensity of p -polarised light when the direction of the external static magnetic field is changed from the saturated state $+M_s$ to $-M_s$, being M_s the saturation magnetisation [1]. The attainment of a large TMOKE response is important for many practical applications that include, but not limited to, 3D imaging [2], magnonics [3, 4], and MO data storage [1].

The natural TMOKE response of continuous single magnetic thin-films is weak and its detection is challenging. Consequently, a large and growing body of research investigates different mechanisms of the enhancement of the TMOKE in thin-film multilayers [5], magneto-plasmonic crystals [6–11], and nanoantennas [12, 13]. All nanostructures mentioned above consist solely of ferromagnetic and nonmagnetic (e.g., gold) metals or contain a nonmagnetic metal nanostructure combined with a magneto-insulating layer.

Pure ferromagnetic magneto-plasmonic nanostructures made, e.g., of nickel (Ni) or permalloy (Py=Ni₈₀Fe₂₀) [8, 9, 12, 13] are gaining increasing attention due to their potential for integration with microwave magnonics devices (magnons are the quanta of magnetisation precession in ferromagnetic media). For instance, pure ferromagnetic nanostructures – magnonic crystals – are used in magnonics for the manipulation of spin waves [3, 4]. The standard techniques with which to read-out information carried by spin waves are the MO Kerr effect (MOKE) and Brillouin light scattering (BLS) spectroscopy. However, the natural interaction between light and dynamic magnetisation is weak because the frequency of the precession of magnetisation (1 – 50 GHz) and the velocity of spin waves ($\sim 3 \times 10^3$ m/s) are widely disparate from those of light (450 – 590 THz and $\sim 3 \times 10^8$ m/s). Thus, the MOKE and BLS spectroscopy will benefit from the increase of the TMOKE response.

The enhancement of the TMOKE response is challenging not only due to the weak interaction of light with magnetic matter. In magneto-plasmonic nanostructures the enhanced TMOKE response is compromised by a relatively low reflectivity of $\sim 20 - 25\%$ (see, e.g., [8, 11]). Furthermore, the maximum of the TMOKE response occurs at the frequency of the Fano resonance [9]. Due to the asymmetry of the line shape of Fano resonances the maximum of the

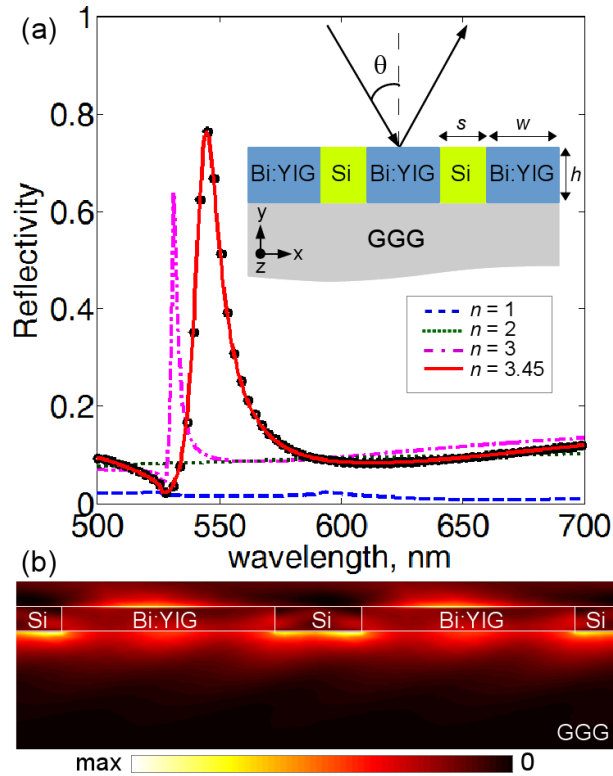


Fig. 1. (a) Inset: Schematic of the proposed grating. The grating is infinite along the z -axis, $h = 100$ nm, $w = 264$ nm, and $s = 113$ nm. Main panel: Reflectivity of the *nonmagnetic* grating calculated for different values of the refractive index n of the material filling the grooves between the Bi:YIG nanostripes. The grating is illuminated by p -polarised light incident at angle $\theta = 35^\circ$. Lines - in-house Rigorous Coupled-Wave Analysis (RCWA) software. Dots - commercial CST Microwave Studio software for $n = 3.45$. (b) The total intensity profile in the plane of incidence at $\theta = 35^\circ$ at the frequency corresponding to the maximum of reflectivity for $n = 3.45$.

TMOKE response is often shifted from the maximum of the reflectivity towards its minimum.

In this paper, we demonstrate theoretically a large TMOKE response in subwavelength gratings consisting of alternating magneto-insulating and nonmagnetic dielectric nanostripes. Without loss of generality, as the magneto-insulating material we employ yttrium iron garnet doped with bismuth (Bi:YIG). As a dielectric material we choose silicon (Si). Whereas Bi:YIG is known to exhibit large MO activity, the high-refractive-index Si nanostripes help to achieve high reflectivity. Also, absorption losses in Bi:YIG and Si are very low as compared with non-magnetic and ferromagnetic metals. As a result, the proposed grating offers a large TMOKE response accompanied by a remarkably high ($\sim 96\%$) resonant reflectivity.

It is noteworthy that other iron garnets with a comparable refractive index, such as YIG that has been used in magnonics for decades [4], can be employed to achieve the main result of this work. Thus, our grating can also serve as a magnonic crystal with simultaneously optimal magnetic and optical properties essential for the enhancement of the MOKE and BLS spectroscopy.

In subwavelength gratings with period significantly smaller than the wavelength of incident light, *at the resonance wavelength* the zero-order reflected and transmitted light is present in the far field, with higher-order diffraction modes suppressed. The high reflectivity exhibited by

subwavelength gratings depends on the angle of incidence and it is attributed to the excitation of a waveguide mode through phase matching by the grating. The waveguide mode then recouples back (again through grating phase matching) to radiative modes and produces the observed high reflection [14–19]. The recoupling occurs at the frequencies of the resonant Wood’s anomaly [14, 15], which in turn is linked to the Rayleigh wavelength at the given angle of incidence. Furthermore, the line shape of the resonance peaks in the reflectivity spectrum of the grating is asymmetric due to Fano interference [14, 20].

The complex resonance behaviour of the proposed subwavelength dielectric grating is a mechanism that differs it from conventional MO diffraction gratings having a large period as compared with the wavelength of incident light [21]. Moreover, similar to magneto-plasmonic gratings, the reflectivity of conventional MO gratings is low. The potential of subwavelength dielectric nanostructures to enhance the MO Kerr effect has been confirmed in [22, 23]. It has been shown that the polar and longitudinal configurations of the MO Kerr effect [1], which are different from the TMOKE, can be enhanced without losing in reflectivity.

2. Results and discussion

The inset in Fig. 1(a) shows the schematic of the proposed subwavelength dielectric grating and defines its dimensions along with the polarisation of light incident at angle θ . The grating consists of alternating nanostripes made of yttrium iron garnet doped with bismuth (Bi:YIG) and silicon (Si). The Bi:YIG–Si periodic structure sits on top of a gadolinium gallium garnet (GGG) layers that needs to be used as a seed substrate for the growth of realistic Bi:YIG nanostructures (see, e.g., [24]). The typical refractive index of Bi:YIG and GGG is $n_{\text{Bi:YIG}} = 2.2 + 0.0011i$ and $n_{\text{GGG}} = 1.97$, correspondingly [25]. Because the refractive index contrast between Bi:YIG and GGG is low, in the absence of the Si nanostripes our in-house RCWA software [26] predicts the reflectivity of the grating of just 2% at $\theta = 35^\circ$ (Fig. 1). This result shows the crucial and adverse impact of the GGG substrate on optical properties of realistic iron garnet nanostructures.

However, at $n = 3.45$ corresponding to Si, we observe that the reflectivity reaches $\sim 78\%$. This result is confirmed by CST Microwave Studio software implementing a Finite Integration Technique. Figure 1(b) shows the intensity profile in the plane of incidence at $\theta = 35^\circ$ at the frequency corresponding to the maximum of reflectivity of the Bi:YIG–Si grating.

Because our RCWA software [26] cannot simulate gyrotropic materials we use CST Microwave Studio to investigate the enhancement of the TMOKE associated with the resonance of the Bi:YIG–Si grating. In the TMOKE configuration the static magnetic field is perpendicular to the plane of incidence. We use the conventional expression [1] to quantify the TMOKE response: $\delta = R(+M_s) - R(-M_s)$, where R denotes the reflectivity. We do not normalise δ to the reflectivity $R(0)$ because in many practical applications (e.g., in magnonics [3]) one measures the difference between $R(+M_s)$ and $R(-M_s)$ without knowing $R(0)$. We also avoid artificial enhancement of the TMOKE that can appear when $R \rightarrow 0$. The reflectivity R changes due to the magnetic field induced change of the boundary conditions at the surface of the Bi:YIG nanostripes of the grating [1, 7]. In simulations, the dielectric permittivity tensor $\epsilon(M_s)$ has the following nonzero components: $\epsilon_{11} = \epsilon_{22} = \epsilon_{33} = n_{\text{Bi:YIG}}^2$, $\epsilon_{13} = ig$, and $\epsilon_{31} = -ig$, where g is the value of the gyration. For a saturated magnetisation $g_{\text{Bi:YIG}} = 0.005$ [25].

The solid line in Fig. 2(a) shows the reflectivity spectrum of the Bi:YIG–Si grating. By changing the sign of the gyration in the dielectric permittivity tensor we simulate the change from $+M_s$ to $-M_s$. The solid line in Fig. 2(b) shows the corresponding TMOKE response δ . We compare these results with the reflectivity and TMOKE response of a continuous Bi:YIG film of the thickness h situated on top of the GGG substrate (the dashed lines in both panels of Fig. 2). We observe a two orders of magnitude enhancement of the TMOKE response of the grating as compared with the continuous film.

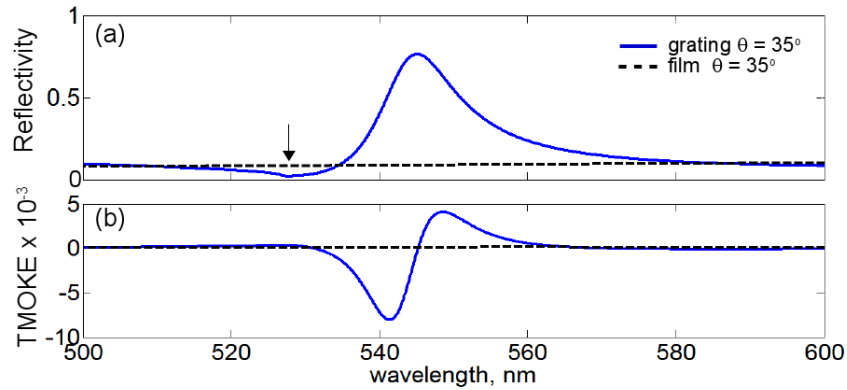


Fig. 2. Reflectivity (a) and TMOKE response (b) of the continuous Bi:YIG film (dashed lines) and Bi:YIG-Si grating (solid lines) at $\theta = 35^\circ$. The Rayleigh wavelength is indicated by the arrow in (a).

The resonance in the reflectivity spectrum of the grating is due to the excitation of a waveguide mode and its recoupling back to the incident region. Both processes occur through phase matching by the grating and they are correlated with the Rayleigh wavelength and diffraction modes of the grating [15]. The Rayleigh wavelength corresponds to the Wood's anomaly, which is due to one of the spectral orders appearing or disappearing in the case of the diffracted wave lying in the plane of the grating. Although the Wood's anomalies are usually associated with the resonant excitation of surface plasmons [8], they are also present whenever there exists a surface mode. Our simulations show that the grating supports a surface wave propagating along the Bi:YIG-Si nanostructure [Fig. 1(b)]. The intensity of the surface wave is higher in the high refractive index Si regions, which additionally confirms the crucial role of the Si nanostructures.

Figure 3(a) shows the sharp resonance peaks in the reflectivity spectra of the grating. The resonance wavelength of the peaks shifts as a function of θ . At $\theta = 25^\circ$, 15° and 10° the first-order reflected (DE_R) and transmitted (DE_T) diffraction efficiency of the grating is zero at the resonance wavelength [Figs. 3(b)–3(d)]. However, $DE_T \neq 0$ at off-resonance wavelengths [Figs. 3(c)–3(d)]. At $\theta = 35^\circ$ at the resonance wavelength DE_R and DE_T are non-zero, but small as compared to the reflectivity [Fig. 3(a)]. This is because at $\theta = 35^\circ$ the resonance occurs at the wavelengths comparable with the grating period and the grating shows the diffraction effect typical of conventional MO gratings [21]. Hence, the higher-order diffraction modes are not fully suppressed.

The linewidth of the resonance peaks gets narrower and the reflectivity increases from 78% to remarkably high 96% as θ is decreased [Fig. 3(a)]. Most significantly, the TMOKE response reaches considerable $\delta = -0.04$ at $\theta = 10^\circ$ [Fig. 3(e)]. Indeed, in accord with the expression quantifying the TMOKE response δ , a shift in the position of a narrow resonance peaks gives rise to a higher TMOKE response than the same shift in the position of a broad peak.

Finally, we refer to Fig. 3(a) in our work [9] where we investigate a Py grating of the same period as the Bi:YIG grating. However, instead of Si the Py grating has air grooves. One can see that at $\theta = 35^\circ$ the TMOKE response of the Py grating is 3.2 times lower as compared with that of the Bi:YIG-Si grating. Furthermore, the reflectivity of the Py grating is $< 20\%$ at the frequency corresponding to the maximum of the TMOKE response.

Under the assumption that Si nanostructures are lossless, our simulations predict that at the resonance the absorption losses in the Bi:YIG-Si grating constitute $\leq 5\%$. In the off-resonance regime the losses are $\sim 0.1\%$. Even though in reality there will be always more losses due to

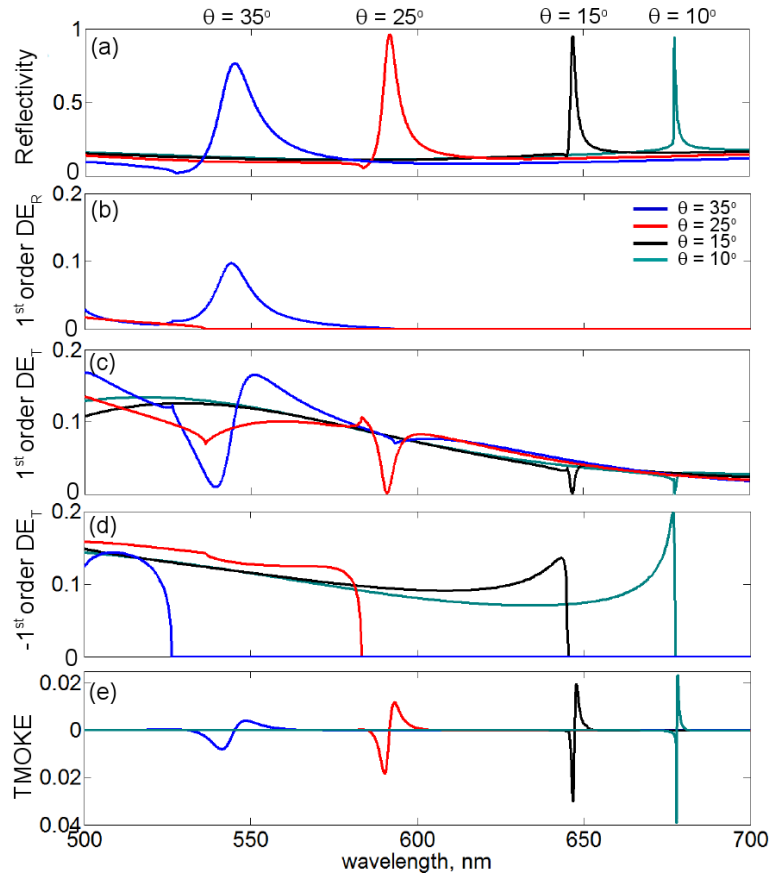


Fig. 3. (a) Reflectivity and (b–d) reflected (DE_R) and transmitted (DE_T) diffraction efficiency for the $+1^{\text{st}}$ and -1^{st} orders of the Bi:YIG–Si grating at different θ . (e) TMOKE response of the grating at different θ . The minor secondary peaks in the spectra occur at the Rayleigh wavelengths.

the effect of the substrate and possible fabrication imperfection, the Bi:YIG–Si grating will always outperform magneto-plasmonic gratings in terms of absorption losses. For instance, at the resonance the losses in the aforementioned Py grating constitute $\sim 65\%$. For further comparison, in a nonmagnetic gold grating of the same geometry the losses are $\sim 25\%$.

3. Conclusions

We have proposed and verified numerically an efficient mechanism of the enhancement of the TMOKE in subwavelength dielectric gratings. We have demonstrated a large TMOKE response accompanied by a very high reflectivity. This result is not readily attainable using magneto-plasmonic gratings. We envision the application of the proposed grating in a variety of devices for high-definition imaging, magneto-optical data storage, and magnonics.

Acknowledgments

This work was supported by the UWA UPRF scheme and Australian Research Council.